第四十屆中華民國電力工程研討會 暨
第十六屆台灣電力電子研討會
台灣 高雄市 2019 年 9 月 5-6 日

牽引系統之 Roof-Delta 結線變壓器塑模與分析

Modeling and Analysis of Roof-Delta Connection Transformer for Traction System

池欣慶	黃維澤	林韋辰
Hsin-Ching Chih	Wei-Tzer Huang	Wei-Chen Lin
姚凱超	吳志鴻	羅鉦彥
Kai-Chao Yao	Chih-Hong Wu	Zheng-Yan Luo
蕭櫂賢	周佳瑩	蘇宸弘
Zhao-Xian Xiao	Chia-Ying Chou	Chen-Hong Su

國立彰化師範大學 工業教育與技術學系
Department of Industrial Education and Technology, National Changhua University of Education
Changhua City, Taiwan, R.O.C.

摘要

本文探討日本最新之鐵道系統 Roof-Delta 牽引變壓器特性。依據變壓器繞組連接方式，推導電壓與電流之關係式，進而獲得 Roof-Delta 牽引變壓器電路模型；接者，採用開源軟體將所推導牽引變壓器模型以 SPICE 與 Python 進行建模與分析，模擬分析所得結果經驗證符合數學方程式解。本文所推導之電路模型可應用於牽引電力系統之模擬分析。

關鍵詞：鐵道系統, 牽引, Roof-Delta 變壓器, Python, SPICE

Abstract

This study aims to explore the characteristics of the Roof-Delta connection traction transformer in Japan high-speed railway system. From its winding connection relationship, it presents the voltage and current phasor equations and diagram. The proposed SPICE-Python hybrid simulation method offers the voltage and current waveforms in an open-source software tool. The derived circuit model in SPICE and Python is capable of simulation and analysis in traction power systems.

Keywords: railway system, traction, Roof-Delta transformer, Python, SPICE

I. Introduction

Railway traction power system is a classic topic since 1908[1]. In between, the traction purpose AC transformers serve to convert the three-phase power source into two single-phase power source for trains operation.

Popular types are Scott connection[2], Le Blanc connection[3, 4], Wood-bridge connection, modified Wood-bridge connection[5] and latest Roof-Delta connection.

Japan replaces the transformers of their high-speed railway system (新幹線/Shinkansen) from modified Woodbridge connection (since 1972 March) to Roof-Delta connection (since 2010 End)[6-8] in the newly built traction stations. This new transformer type has various features, such as less winding numbers, smaller installation location space, light net weight, less volume of cooling oil, more efficient radiators, and diminished loss[9].

This study involves the Roof-Delta transformer connection, characteristic, and SPICE (Simulation Program with Integrated Circuit Emphasis) simulation in the following session.

II. Roof-Delta connection traction transformer

A Roof-Delta multi-winding connection system diagram [10-12] is in Fig. 1. The transformer consists of three major winding sets in Primary, Secondary A-set, and B-set side. The Secondary A-set is in open-wye connection with 0.577 ($1/\sqrt{3}$) turning number ratio in compare with B-set. The B-set is the typical Delta connection transformer. The Primary -side connection is the wye-connection format. Converted power sources (DB and CA) serve two independent trains operation in AT (Auto Transformer) feeding method.

The significant difference between the modified Wood-bridge connection is no external step-up transformer. A comparison with clear illustration from Iketo study is in Fig 2[12]. The new transformer saves the facility space and operation cost. Kamio[13] study exhibits the numbers of winding in the Modified Woodbridge connection is 16. In contrast, Roof-Delta connection only requires in 8. Furthermore, it can execute a “ground connection” process rather than the Scott connection.

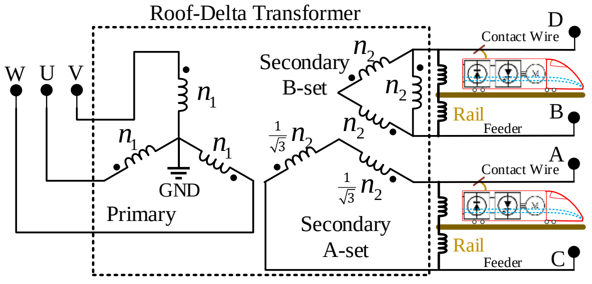

Fig. 1 Connection in the roof-delta traction transformer and AT feeding for two-train service operation Railway

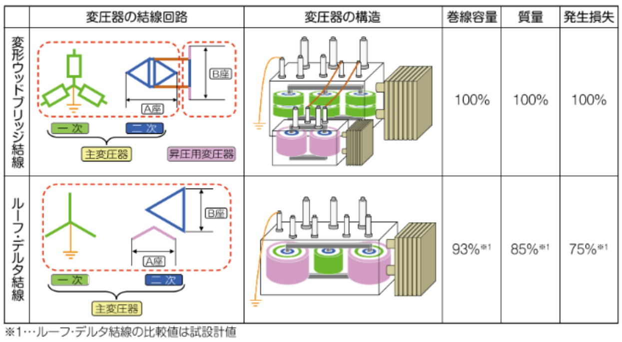

	変圧器の結線回路	変圧器の構造	巻線容量	質量	発生損失
変形ウッドブリッジ結線			100%	100%	100%
ルーフ・デルタ結線			93%※1	85%※1	75%※1

※1…ルーフ・デルタ結線の比較値は試設計値

Fig. 2 Comparison with the modified Wood-bridge connection transformer (Top) and Roof-Delta connection transformer (Bottom) from Iketo[12]

III. Circuit Model Derivation

This session explores the voltage and current input and output side equations for its behavior investigation. The transformer's current flow is in below Fig. 3[10].

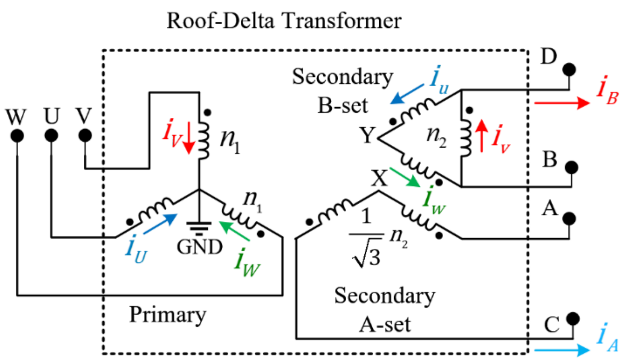

Fig. 3 Roof-Delta transformer current flow chart

The input three-phase power V_W V_V and V_U line-to-line voltage represent[11] in

$$V_W = V_P\angle(4\pi/3) \quad (1)$$

$$V_V = V_P\angle(0) \quad (2)$$

$$V_U = V_P\angle(2\pi/3) \quad (3)$$

Where, V_P is the Primary side line-to-line rms voltage. Each winding voltage in the Secondary side A-set are

$$V_{AX} = \left(\frac{1}{\sqrt{3}} n_2 / n_1\right)\left(V_p/\sqrt{3}\right)\angle(4\pi/3) \quad (4)$$

$$V_{CX} = \left(\frac{1}{\sqrt{3}} n_2 / n_1\right)\left(V_p/\sqrt{3}\right)\angle(2\pi/3) \quad (5)$$

Hence, converted power sources in B-set (V_{DB}) and A-set (V_{CA}) voltage vector are

$$V_{DB} = (n_2/n_1)\left(V_p/\sqrt{3}\right)\angle(0) \quad (6)$$

$$V_{CA} = (V_{CX} - V_{AX}) = (n_2/n_1)\left(V_p/\sqrt{3}\right)\angle(\pi/2) \quad (7)$$

From (6-7), the dual-source is in the 90-degree phase shift characteristic. Fig. 4 illustrates the phasor diagram.

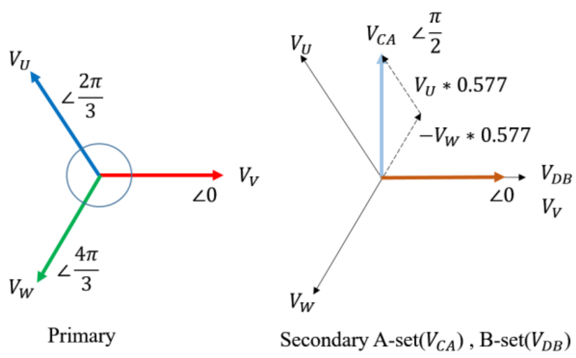

Fig. 4 Voltage phasor diagram in Primary and two Secondary sides

In B-set [11], current flow relation is in

$$i_u = i_v - i_B \quad (8)$$

$$i_u = i_w \quad (9)$$

Regarding turn ratio between Primary and Secondary B-set, the current flow relation is in

$$i_U = (n_2/n_1)\left(i_u + \left(1/\sqrt{3}\right) i_A\right) \quad (10)$$

$$i_W = (n_2/n_1)\left(i_w - \left(1/\sqrt{3}\right) i_A\right) \quad (11)$$

Substitute (10-11) by (8-9) and derive in

$$i_U = (n_2/n_1)\left(i_v - i_B + \left(1/\sqrt{3}\right) i_A\right) \quad (12)$$

$$i_W = (n_2/n_1)\left(i_v - i_B - \left(1/\sqrt{3}\right) i_A\right) \quad (13)$$

Add (12) and (13) into (14)

$$i_U + i_W = (n_2/n_1)(2i_v - 2i_B) \quad (14)$$

Given a balanced wye-connection power system, it satisfies (15).

$$i_W + i_U = -i_V \tag{15}$$

Replaces (14) by (15) and derives as

$$i_V = (n_2/n_1)(2/3)i_B \tag{16}$$

Substitute (12-13) by (16), the current are in below.

$$i_U = (n_2/n_1)\left(-(1/3)i_B + \left(1/\sqrt{3}\right)i_A\right) \tag{17}$$

$$i_W = (n_2/n_1)\left(-(1/3)i_B - \left(1/\sqrt{3}\right)i_A\right) \tag{18}$$

Eqs. (16-18) are the transformer current flow equations between the Primary side and the dual Secondary sides. Current i_A and i_B are in the 90-degree phase from (4-5). Assume $|i_A| = |i_B|$ condition, the Primary side input current summarizes in below.

$$i_W = (n_2/n_1)(2/3)i_B\angle(4\pi/3) \tag{19}$$

$$i_V = (n_2/n_1)(2/3)i_B\angle(0) \tag{20}$$

$$i_U = (n_2/n_1)(2/3)i_B\angle(2\pi/3) \tag{21}$$

IV. Simulation and Discussion

This study adopts the “SPICE+Python” hybrid method from a previous study[12]. It advantages in the open-source software, GPU (Graphics Processor Unit) parallel computation capability and time base node data for the transient state, steady state, and harmonics component analysis features. The single-phase transformer SPICE model, AT (auto-transformer) element and the Scott connection transformer application, is in the previous study[13]. Fig. 5 illustrates the Roof-Delta connection hybrid model in the simulation. The n_1 and n_2 transformer turn ratio factor is the same.

Fig.6 and Fig. 7 are the simulation result. The secondary side induces a half-voltage in 19.044 kVrms with a 90° phase shift. The Primary side supplies 66 kVrms–50 Hz three-phase power. The waveform is identical to Fig. 14 of [14]. This voltage value is in half of Eqs. (6-7). It is because of utilizing the AT feeding in the traction system.

Each single-phase loading consumes 211.6 A current, thereby resulting in a Primary-side phase current of 141.0 A in balance load scenario. It satisfies with Eqs. (19-21).

The overall three-phase conversion power values on the Primary and Secondary sides are 16.123292 MW and 16.1232164 MW, respectively, for prove correction.

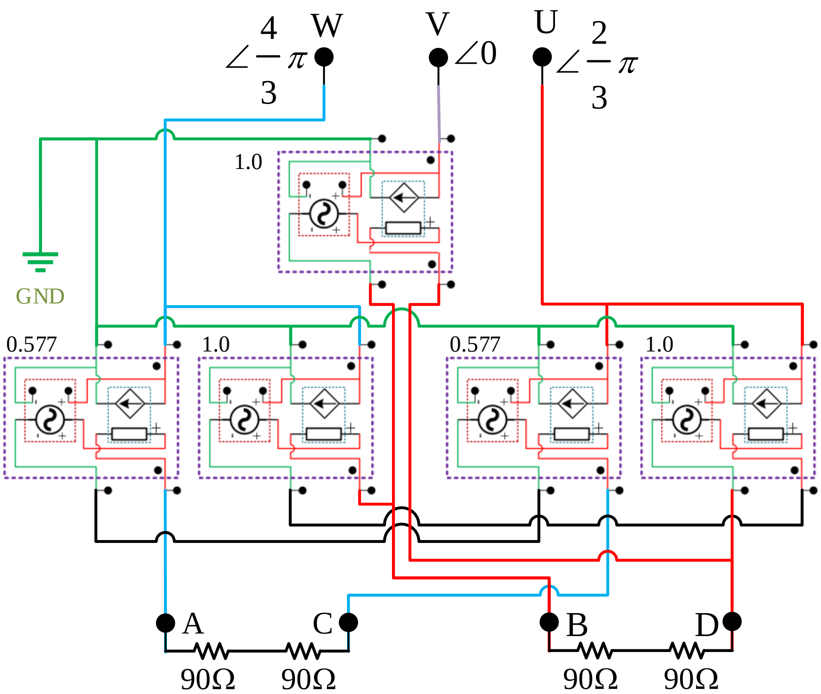

Fig. 5 “SPICE+Python” model with dual 180Ω loading

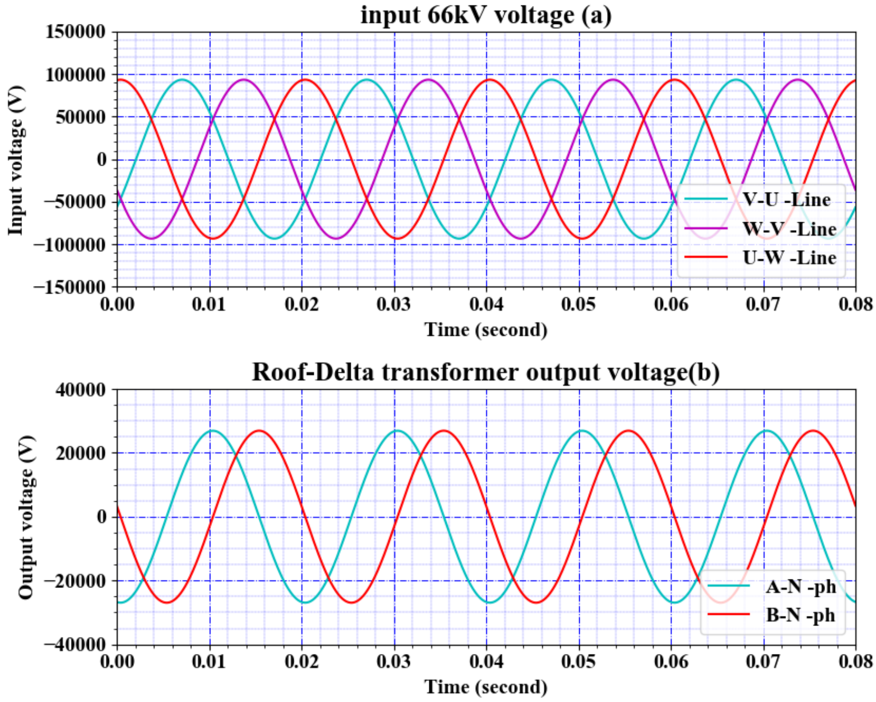

Fig. 6 Primary (top) and dual Secondary (bottom) half-voltage waveform comparison in Roof-Delta connection transformer.

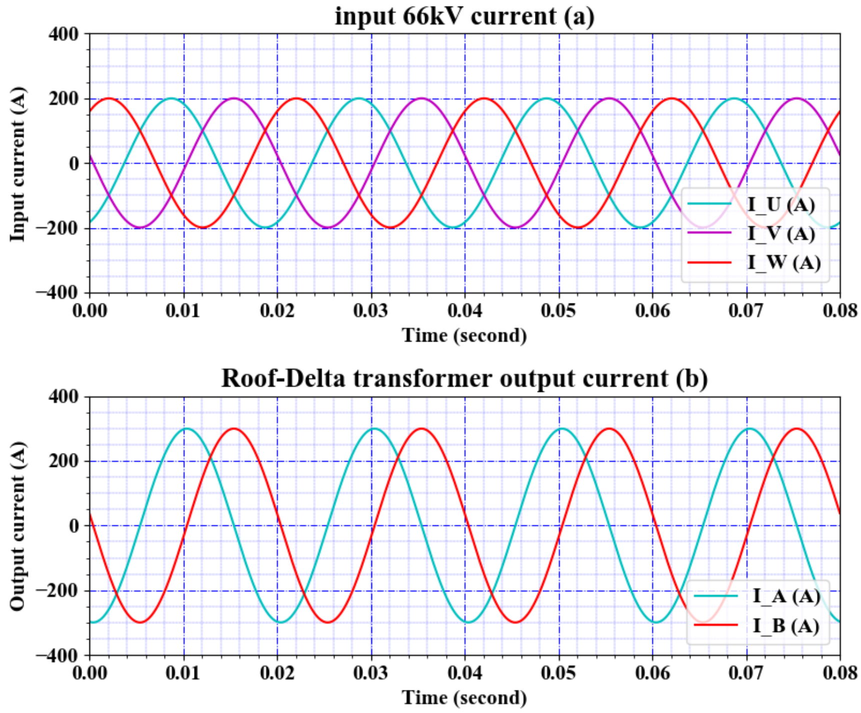

Fig. 7 Primary (top) and dual Secondary (bottom) current waveform comparison in Roof-Delta connection transformer

IV. CONCLUSIONS

This study introduced the latest multi-phase traction transformer in Japan high-speed railway system. The comparison commented in its connection topology and strength. Both voltage and current phasor equations of the transformer were derived. The "SPICE+Python" hybrid method simulated the proposed model and plotted waveforms. In simulation result, a 66kVrms-50Hz system converted into two 19.044kVrms with a 90-degree shift.

Dual single-phase loading consumes 211.6 A current, thereby resulting in a Primary-side phase current of 141.0 A. All these results meet the proposed equation in (6-7) and (19-21). This ideal transformer conversion efficiency is almost 100%.

ACKNOWLEDGMENT

Authors would like to thank the Ministry of Science and Technology of Taiwan under MOST 107-2221-E-018-013 - for this paper achievement.

REFERENCES

[1] J. E. Woodbridge, "Some features of railway converter design and operation," *Proceedings of the American Institute of Electrical Engineers,* vol. 27, no. 2, pp. 203-226, 1908.

[2] A. C. Franklin and D. P. Franklin, "7 - Polyphase connections," in *The J & P Transformer Book (Eleventh Edition)*, A. C. Franklin and D. P. Franklin, Eds.: Butterworth-Heinemann, 1983, pp. 136-172.

[3] H. Sy Ruen, K. Yueh Lung, C. Bing Nan, L. Kwang Chang, and H. Min Chuian, "A short circuit current study for the power supply system of Taiwan railway," *IEEE Transactions on Power Delivery,* vol. 16, no. 4, pp. 492-497, 2001.

[4] H. Sy-Ruen and C. Bing-Nan, "Harmonic study of the Le Blanc transformer for Taiwan railway's electrification system," *IEEE Transactions on Power Delivery,* vol. 17, no. 2, pp. 495-499, 2002.

[5] Y. Oura, Y. Mochinaga, and H. Nagasawa, "Railway Electric Power Feeding Systems," *Japan Railway & Transport Review,* vol. 16, 1998.

[6] 杉井守, "明電舎の変電事業について," 2016, Available: https://www.meidensha.co.jp/news/news_03/news_03_01/__icsFiles/afieldfile/2016/05/19/20160519henden.pdf.

[7] T. Yanari, "History of Power Transformers in Japan and Description of Related Historical Materials," 2004.

[8] 清水泉 and 牛山茂樹, "東北・上越新幹線 変電・配電機器更新," *電気設備学会誌-J. IEIE Jpn.* , vol. 31, no. 6, p. 4, 2011.

[9] 森本大観, "新型(ルーフ・デルタ)結線変圧器," *RRR,* p. 1, 2008.

[10]K. Kawakaki, T. Koshizuka, S. Maruyama, M. Saito, and N. Nagayama, "Magnetizing inrush current suppression device and suppression method therefor," Japan, 2014. Available: https://astamuse.com/ja/published/JP/No/2014023308.

[11]D. Oyamatsu. (2019). *三相交流から単相交流への変換 スコット結線・変形ウッドブリッジ結線・ルーフデルタ結線*. Available: http://deadsection.image.coocan.jp/dead_sec/conv3-2/conv3-2.htm

[12]H. Vogt, M. Hendrix, and P. Nenzi, "Ngspice Users Manual ngspice-28," 2018, Available: http://sourceforge.net/projects/ngspice/files/.

[13]W.-T. Huang, H.-C. Chih, and K.-C. Yao, "Scott Connection Transformer Analysis in the Railway Traction System Using the Simulation Program with Integrated Circuit Emphasis Model," in *IEEE International Conference on Power Electronics and Drive Systems*, Toulouse, France, 2019, p. 3.

[14]H. Morimoto, T. Uzuka, A. Horiguchi, and T. Akita, "New type of feeding transformer for AC railway traction system," in *2009 International Conference on Power Electronics and Drive Systems (PEDS)*, 2009, pp. 800-805.